*Published online 5 October 2006* *Nucleic Acids Research, 2006, Vol. 34, No. 19* ***5613–5622***
*doi:10.1093/nar/gkl717*

# Effects of the trinucleotide preceding the self-cleavage site on eggplant latent viroid hammerheads: differences in co- and post-transcriptional self-cleavage may explain the lack of trinucleotide AUC in most natural hammerheads

**Alberto Carbonell, Marcos De la Peña, Ricardo Flores* and Selma Gago**

Instituto de Biología Molecular y Celular de Plantas (UPV-CSIC), Avenida de los Naranjos, s/n, 46022 Valencia, Spain

Received August 1, 2006; Revised September 15, 2006; Accepted September 16, 2006

## ABSTRACT

**Eggplant latent viroid (ELVd) can form stable hammerhead structures in its (+) and (−) strands. These ribozymes have the longest helices I reported in natural hammerheads, with that of the ELVd (+) hammerhead being particularly stable (5/7 bp are G-C). Moreover, the trinucleotide preceding the self-cleavage site of this hammerhead is AUA, which together with GUA also found in some natural hammerheads, deviate from the GUC present in most natural hammerheads including the ELVd (−) hammerhead. When the AUA trinucleotide preceding the self-cleavage site of the ELVd (+) hammerhead was substituted by GUA and GUC, as well as by AUC (essentially absent in natural hammerheads), the values of the self-cleavage rate constants at low magnesium of the purified hammerheads were: ELVd-(+)-AUC≈ELVd-(+)-GUC>ELVd-(+)-GUA> ELVd-(+)-AUA. However, the ELVd-(+)-AUC hammerhead was the catalytically less efficient during *in vitro* transcription, most likely because of the transient adoption of catalytically-inactive metastable structures. These results suggest that natural hammerheads have been evolutionary selected to function co-transcriptionally, and provide a model explaining the lack of trinucleotide AUC preceding the self-cleavage site of most natural hammerheads. Comparisons with other natural hammerheads showed that the ELVd-(+)-GUC and ELVd-(+)-AUC hammerheads are the catalytically most active in a post-transcriptional context with low magnesium.**

## INTRODUCTION

Hammerhead ribozymes were initially described in viroid and viroid-like satellite RNAs wherein they mediate self-cleavage of the multimeric RNA intermediates of one or both polarities resulting from replication through a rolling-circle mechanism [(1,2), for a review see Ref. (3)]. More specifically, hammerhead viroids follow a symmetric pathway of this mechanism in which the multimeric RNAs of both polarities self-cleave and subsequently are ligated into the corresponding monomeric circular RNAs (4). Early structural dissection showed that minimized catalytically-active hammerheads have as few as 52 nt (5,6), igniting much interest in deciphering the catalytic mechanism (7–9) and developing its potential as a biotechnological tool (10). Most natural hammerheads are formed by a central conserved core flanked by three double-stranded regions with relaxed sequence requirements (helices I, II and III), two of which (I and II) are capped by short loops (1 and 2, respectively). X-ray crystallography uncovered an intricate assortment of non-canonical interactions between the nucleotides of the central core, explaining their conservation in natural hammerheads and illustrating that the actual contour does not resemble a hammerhead but rather a distorted Y in which the basal helix III is almost co-linear with helix II, whilst helix I forms an angle (7–9).

However, these structural studies, which were performed with artificial hammerheads, are partially at odds with some biochemical data (11), and the use of artificial ribozymes designed to act in *trans* against specific RNA targets have met with limited success *in vivo*. More recent data have provided an explanation for these discrepancies by showing that modifications of loops 1 and 2 of natural hammerheads provoke a drastic reduction in their catalytic activity, indicating that these peripheral regions play a crucial role in catalysis through tertiary interactions between some of their nucleotides that may favor the active site at the low magnesium concentration

*To whom correspondence should be addressed. Tel: +34 96 3877861; Fax: +34 96 3877859; Email: rflores@ibmcp.upv.es

© 2006 The Author(s).
This is an Open Access article distributed under the terms of the Creative Commons Attribution Non-Commercial License (http://creativecommons.org/licenses/by-nc/2.0/uk/) which permits unrestricted non-commercial use, distribution, and reproduction in any medium, provided the original work is properly cited.

existing *in vivo* (12–15). These interactions, direct evidence for which has been recently derived from the crystallographic structure of a natural hammerhead (16), are currently being incorporated into a new generation of more efficient *trans*-acting artificial hammerheads (17–19).

Eggplant latent viroid (ELVd) (20) is the last reported member of the family *Avsunviroidae* of hammerhead viroids (4,21). Both (+) and (−) ELVd hammerheads display some peculiarities, the influence of which in the catalytic behavior of these ribozymes has not yet been determined. Here we report the effects of changes in the trinucleotide preceding the self-cleavage site on the self-cleavage kinetics of the ELVd hammerheads, together with a model explaining the lack of trinucleotide AUC in most natural hammerheads, based on differences in co- and post-transcriptional self-cleavage. We also present a comparative analysis of the ELVd hammerheads with other natural hammerheads in a post-transcriptional context at low magnesium concentrations.

## MATERIALS AND METHODS

### Construction of hammerhead cDNAs

The cDNA of the ELVd (+) hammerhead was PCR-amplified with *Pwo* DNA polymerase and the buffer recommended by the supplier (Roche Diagnostics) using as template the plasmid containing the complete cDNA of the ELVd reference variant (ELVd-2) (20) and the sense RF-689 (5′-TAATACGACTCACTATAGGCCCCATAGGGTGGTGTG-3′) and antisense RF-690 (5′-*TCTAGA*CCCCATTTCGACC-3′) primers. Mutants of the trinucleotide preceding the self-cleavage site were obtained by PCR amplification using the same template and the sense RF-691 (5′-TAATACGACTCACTATAGGCCCCgTcGGGTGGTGTG-3′) and antisense RF-692 (5′-*TCTAGA*CCCCgTTTCGACC-3′) primers for the hammerhead with the trinucleotide GUC, the sense RF-693 (5′-TAATACGACTCACTATAGGCCCCATcGGGTGGTG-TG-3′) and antisense RF-690 primers for the hammerhead with the trinucleotide AUC, and the sense RF-694 (5′-TAATACGACTCACTATAGGCCCCgTAGGGTGGTGTG-3′) and antisense RF-692 primers for the hammerhead with the trinucleotide GUA. After an initial denaturation at 94°C for 2 min, the PCR profile (30 cycles) was: 94°C for 20 s, 60°C for 30 s and 72°C for 30 s, with a final extension at 72°C for 10 min. The cDNA of the (+) hammerhead of the satellite RNA of tobacco ring spot virus (sTRSV) was prepared by extension of the partially overlapping sense RF-875 (5′-GGTAATACGACTCACTATAGGCTGTCACC-GGATGTGCTTTCCGGTC-3′) and antisense RF-876 (5′-GGG*TCTAGA*CTGTTTCGTCCTCACGGACTCATCAG-ACCGGAAAGC-3′) primers (five cycles at 94°C for 30 s, 30°C for 30 s and 72°C for 30 s, with a final extension at 72°C for 2 min). Sense primers included the T7 promoter (underlined) and antisense primers the XbaI site (in italics). Point mutations are indicated with lower case letters. PCR products were separated by PAGE in 10% gels and those with the expected length were eluted, digested with XbaI and cloned into pUC18 opened with XbaI and SmaI. Sequencing of the recombinant plasmids confirmed that they contained only the expected mutations. Construction of (+) hammerheads of peach latent mosaic viroid (PLMVd) and chrysanthemum chlorotic mottle viroid (CChMVd) has been reported previously (12).

### Synthesis and purification of hammerhead RNAs

Hammerhead RNAs were generated by *in vitro* transcription of the corresponding recombinant plasmids linearized with XbaI. Transcription reactions (25 μl) contained 40 mM Tris–HCl, (pH 8), 6 mM $MgCl_2$, 2 mM spermidine, 10 mM DTT, 10 mM NaCl, 0.4 mM each of ATP, CTP and GTP, 0.08 mM UTP plus 0.25 μCi/μl [$\alpha$-$^{32}$P]UTP, 0.8 U/μl of rRNasin ribonuclease inhibitor (Promega), 20 ng/μl of plasmid, 1.2 U/μl of T7 RNA polymerase and, when indicated, 0.1–1 mM of the self-cleavage blocking oligodeoxyribonucleotide(s). Blocking oligodeoxyribonucleotides were: RF-122 (12) and RF-88 (5′-CAAGAGTTTCGTCTCATTTC-3′) for PLMVd, RF-142 for CChMVd (12), RF-872 (5′-TCTC-ATCAGGGGTGGCACACAC-3′) and RF-873 (5′-CCCCAT-TTCGACCTTTCG-3′) for ELVd, and RF-890 (5′-ACTCA-TCAGACCGGAAAGCACATC-3′) and RF-891 (5′-CTGT-TTCGTCCTCACG-3′) for sTRSV. After incubation at 37°C for 45 min, transcription products were mixed with an excess of stop solution [50% formamide, 8 M urea, 50 mM EDTA and 0.25% of bromophenol blue and xylene cyanol], heated at 95°C for 1.5 min, and fractionated by PAGE in 15% gels containing 8 M urea. The uncleaved primary transcripts were extracted from the crushed gel pieces with phenol saturated with buffer [Tris–HCl 10 mM, (pH 8), EDTA 1 mM and SDS 0.7%] containing formamide (40%) to prevent self-cleavage, recovered by ethanol precipitation and resuspended in sterile deionized water.

### Self-cleavage kinetics of purified hammerhead RNAs

To determine the self-cleavage rate constants, the purified primary transcripts from the different hammerheads were incubated in 20 μl of 50 mM Tris–HCl, (pH 7.5) for 2 min at 95°C followed by a slow ramp down to 25°C at −6°C/min. Samples were incubated for 5 min at 25°C and, after taking a zero-time aliquot, the reactions were initiated by addition of $MgCl_2$ to the indicated concentrations (10 and 50 μM). Aliquots were removed at appropriate time intervals and quenched with 10 volumes of stop solution at 0°C. After heating at 95°C for 1.5 min, primary transcripts and their cleavage products were resolved by PAGE in 15% gels containing 8 M urea and quantified with a bioimage analyzer. The product fraction at different times ($F_t$) was determined and fitted to the equation $F_t = F_\infty(1-e^{-kt})$, where $F_\infty$ is the product fraction at the endpoint, respectively, and $k$ is the first order rate constant of self-cleavage ($k_{cat}$). Values are the means of three independent experiments.

### Self-cleavage kinetics of hammerhead RNAs during transcription

Reactions, in absence of blocking oligodeoxyribonucleotides, were performed as described above with the exception of the $MgCl_2$ concentration, which was adjusted as indicated in Results, and the T7 RNA polymerase, which was added to trigger the reactions (zero time). Reaction mixtures were pre-incubated at 37°C for 1 min before adding the polymerase and then aliquots were removed at different time intervals

and quenched with 10 volumes of stop solution at 0°C. Quantitation of primary transcripts and their cleavage products was as detailed above, and the self-cleavage rate constants (at 2 mM $MgCl_2$) were determined using the equation derived previously (22). Values are the means of at least two independent experiments.

## RESULTS

### Some peculiarities of the hammerhead structures from ELVd

The detailed morphology of both ELVd hammerheads has been reported previously (20) and, therefore, we will only summarize here their most salient features when compared with other natural hammerheads that have been used in this work. Both (+) and (−) ELVd strands contain the 11 residues that form the central conserved core of natural hammerheads (3), flanked by helix I/loop 1 (7 bp and 4 nt), helix II/loop 2 (4 bp and 4 nt forming a stable loop of the GNRA family) (23,24), and helix III (6 and 5 bp for + and − hammerhead, respectively) (Figure 1 and Table 1). This morphology is similar to that of both hammerheads of PLMVd (25), and to the (+) hammerheads of CChMVd (26) and sTRSV (2) (Figure 1), although helices I of ELVd hammerheads are the longest reported in natural hammerheads (3), with that of the (+) hammerhead being particularly stable (5/7 bp are G–C).

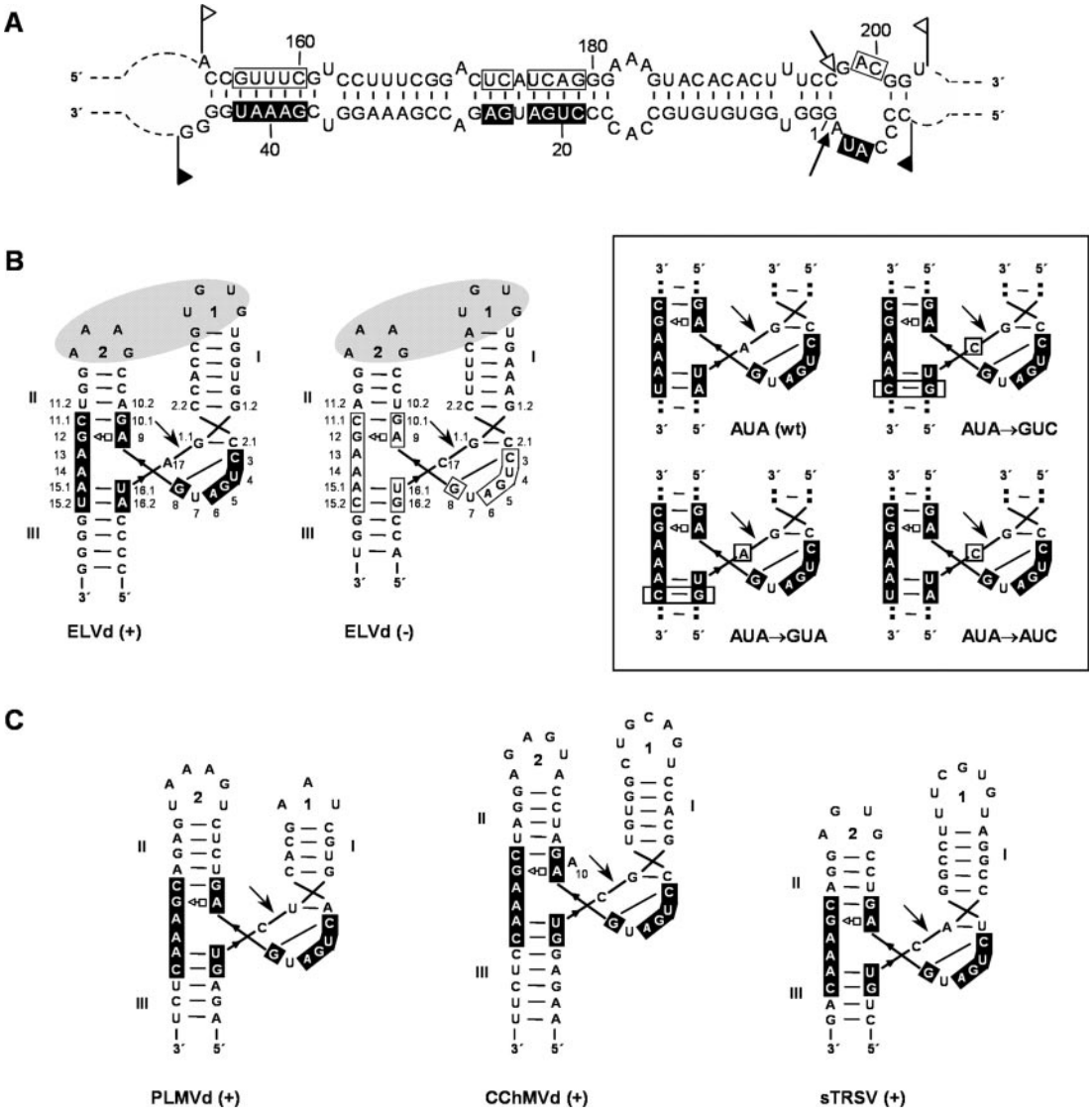


**Figure 1.** (**A**) Rod-like secondary structure that the nucleotides involved in both hammerheads adopt in the predicted most stable conformation of the reference variant of ELVd (+) RNA (accession number AJ536613). Sequences forming the hammerheads are delimited by flags, motifs conserved in most natural hammerheads are within boxes, and self-cleavage sites are marked by arrows. Black and white backgrounds refer to (+) and (−) polarities, respectively. (**B**) Structure of the ELVd (+) and (−) hammerheads according to crystallographic data obtained for the *Schistosoma mansoni* hammerhead (16). Open square next to open triangle denotes Hoogsteen/sugar edge. Numbering of nucleotides and nomenclature of helices and loops is consistent with the standard criterion. Motifs conserved in most natural hammerheads are within boxes, and self-cleavage sites are marked by arrows. Black and white backgrounds refer to (+) and (−) polarities, respectively. The ovals represent the proposed tertiary interactions between loops 1 and 2 that increase the self-cleavage rates. The inset at the right displays the mutants derived from the ELVd (+) hammerhead used in the present work, with the changes introduced within boxes. (**C**) Structure of the (+) hammerheads of PLMVd, CChMVd and sTRSV.

**Table 1.** Structural characteristcs of some hammerhead ribozymes

| Hammerhead | Helix I/ loop 1[a] | Helix II/ loop 2 | Helix III | Trinucleotide preceding the self-cleavage site (5′→3′) |
|---|---|---|---|---|
| ELVd (+) | 7/4 | 4/4 | 6 | AUA |
| ELVd (−) | 7/4 | 4/4 | 5 | GUC |
| ELVd-(+)-GUC | 7/4 | 4/4 | 6 | GUC |
| ELVd-(+)-AUC | 7/4 | 4/4 | 6 | AUC |
| ELVd-(+)-GUA | 7/4 | 4/4 | 6 | GUA |
| PLMVd (+) | 5/3 | 5/6 | 5 | GUC |
| CChMVd (+) | 6/7 | 5/6 | 7 | GUC |
| sTRSV (+) | 6/7 | 4/4 | 4 | GUC |
| cscRNA (+) | 6/6 | 4/4 | 7 | GUA |
| cscRNA (−) | 6/6 | 4/4 | 5 | AUA |
| sLTSV (−) | 6/13 | 4/6 | 5 | GUA |
| sCYDV-RPV (+) | 4/8 | Atypical[b] | 6 | AUA |

[a]Length of helices (in base pairs) and loops (in bases).
[b]Long helix II composed by segments of 5, 4 and 4 bp separated by internal loops and closed by a terminal loop of 4 bases.

The sequence heterogeneity observed in natural ELVd variants is consistent with the existence in helix I of both ELVd hammerheads of a base pair between positions 1.7 and 2.7, because a U–G pair is substituted by a U–A pair or viceversa (20). In the (+) ELVd hammerhead, positions 15.2 and 16.2 form a U–A pair instead of the predominant C–G pair, a situation also found in the (+) hammerhead of satellite RNA of cereal yellow dwarf virus RPV (sCYDV-RPV) (27) and in the (−) hammerhead of two cherry small circular RNAs (csc RNAs) (28,29). In these three hammerheads the residue preceding the self-cleavage site is A and not C (Table 1) as in most natural hammerheads, suggesting some relationship between the three positions (20,28,29). The two ELVd hammerheads are more related to each other than to other hammerheads, as also occurs between the hammerheads of other viroid and viroid-like RNAs (5,25,26,28,29).

### Antisense oligodeoxyribonucleotides against loops 1 and 2 efficiently prevent self-cleavage during *in vitro* transcription of minimal natural hammerheads

Although the self-cleavage rates of artificial hammerheads can be estimated based on measurements from *in vitro* transcription reactions (12,22,30,31), most natural hammerheads self-cleave efficiently under standard *in vitro* transcriptions. This forces the adoption of non-standard conditions, particularly low pH and magnesium concentration (12,31), which complicate further kinetic comparisons between different hammerheads. The alternative approach for estimating hammerhead self-cleavage rates, isolation of the uncleaved RNA from *in vitro* transcriptions and its subsequent incubation in a protein-free buffer (1,32–34), suffers the limitation that the uncleaved primary transcript usually represents a minor fraction of the transcription products. Extensive self-cleavage of the hammerhead RNA during *in vitro* transcription can be avoided by incorporating an oligodeoxyribonucleotide complementary to part of the ribozyme. This approach has been previously used with one ribozyme of hepatitis delta virus RNA (35), with *in vitro* selection of self-cleaving RNAs (36), with the CChMVd (+) and PLMVd (+) hammerheads (12)

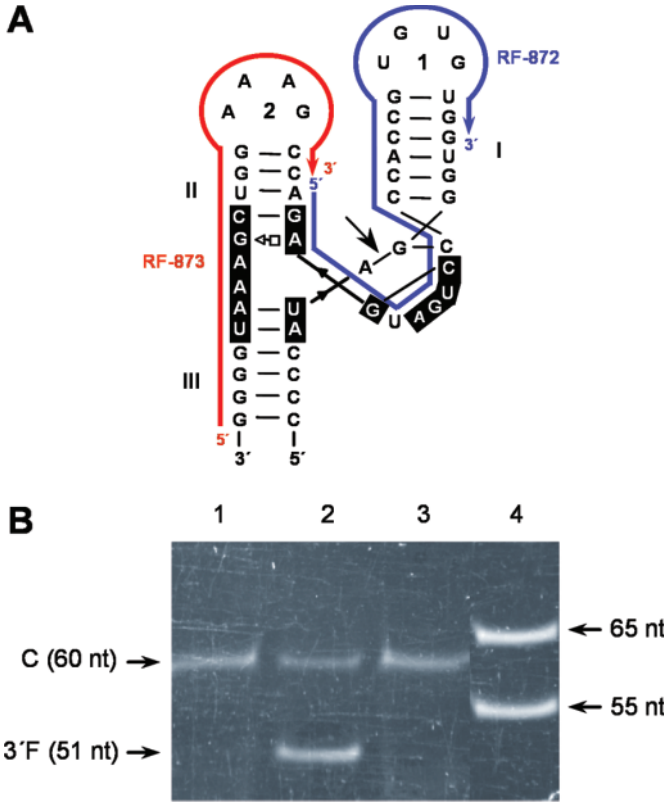


**Figure 2.** (**A**) Positions of the ELVd (+) hammerhead covered by two antisense oligodeoxyribonucleotides (in color). Other details as in the legend to Figure 1. (**B**) Self-cleavage during transcription of the ELVd (+) hammerhead in the presence and absence of the antisense oligodeoxyribonucleotides (lanes 1 and 2, respectively), and of the mutant ELVd-(+)-GUC hammerhead (in which the wild-type AUA trinucleotide preceding the self-cleavage site has been substituted by GUC) in the presence of the antisense oligodeoxyribonucleotides (lane 3). Lane 4, RNA markers of 65 and 55 nt. Aliquots of the reaction mixtures were analyzed by PAGE in 15% gels containing 8 M urea that were stained with ethidium bromide. Positions of the complete (**C**) primary transcript (60 nt) and of the resulting self-cleavage 3′ fragment (3′F) (51 nt) are indicated with arrows. The self-cleavage 5′ fragment (9 nt) migrated out of the gel.

and with certain hammerheads encoded in the genome of *Arabidopsis thaliana* (37). In the CChMVd case, high levels of uncleaved primary transcripts (75% of the total RNA) were obtained in the presence of oligodeoxyribonucleotides complementary to the sequences forming part of helix I/loop 1 and helix II/loop 2 and the connecting CUGAUGA of the conserved central core (12).

Preliminary experiments with the ELVd (+) hammerhead showed that self-cleavage proceeded extensively during *in vitro* transcription under standard conditions (data not shown). In an attempt to attenuate this problem, an antisense oligodeoxyribonucleotide analogous to those used previously with the CChMVd (+) hammerhead (12) was incorporated to the *in vitro* transcription mixture. However, the protecting effects were limited, as also were the effects of two other oligodeoxyribonucleotides complementary to sequences forming part of helix I/loop 1 and helix III connected by the A preceding the self-cleavage site, and to sequences forming part of helix II/loop 2 and helix III (data not shown). Considering that the fast self-cleavage rates of most natural hammerheads

are very much influenced by tertiary interactions between loops 1 and 2 (12–15), we designed two oligodeoxyribonucleotides, one complementary to the complete loop 1 and its adjacent sequences of helices I and II, and the other complementary to the complete loop 2 and its adjacent sequences of helices II and III (Figure 2A). Co-incorporation of the two oligodeoxyribonucleotides to the *in vitro* transcription mixture abolished essentially self-cleavage (Figure 2B, compare lanes 1 and 3 with 2), providing further support for the proposed tertiary interactions between loops 1 and 2. Moreover, the same approach also worked for the PLMVd (+) and sTRSV (+) hammerheads (data not shown), thus indicating that it may be of general application. A possible explanation for these results is that loops 1 and 2 may be more easily accessible to antisense oligodeoxyribonucleotide than regions more structured like the central conserved core or its flanking helices.

### Self-cleavage kinetics of the ELVd (+) hammerhead and of three mutants affecting the trinucleotide preceding the self-cleavage site

The trinucleotide preceding the self-cleavage site of most natural hammerheads, including the ELVd (−) hammerhead, is GUC (3,20). However, there are exceptions to this rule. As already indicated, the trinucleotide preceding the self-cleavage site of the ELVd (+), sCYDV-RPV (+) and csc RNAs (−) hammerheads is AUA (20,27–29). Furthermore, the trinucleotide preceding the self-cleavage site of the (+) hammerhead of csc RNAs and the (−) hammerhead of the satellite RNA of lucerne transient streak virus (sLTSV) is GUA (5,28,29) (Table 1). Because the effects on self-cleavage kinetics of interchanging these trinucleotides preceding the self-cleavage site have not been determined in a *cis* context and at low magnesium concentration, we examined this question in the ELVd (+) hammerhead. As a control, we also studied the effect of the trinucleotide AUC, which with one exception (see below), has never been found preceding the self-cleavage site of natural hammerheads.

At very low magnesium concentration (10 μM), the ELVd-(+)-GUC mutant (where the GUC refers to the trinucleotide preceding the self-cleavage site) presented a self-cleavage rate constant significantly higher than the wild-type ELVd-(+)-AUA hammerhead (Figure 3A). The ELVd-(+)-GUA mutant had a self-cleavage rate constant intermediate between those of the ELVd-(+)-GUC mutant and the ELVd-(+)-AUA wild-type but, surprisingly, the ELVd-(+)-AUC mutant displayed the highest rate constant (Figure 3A). Moreover, at the end-point of the reaction, 95% of molecules from the three mutants with the highest rate constants self-cleaved, whereas this fraction was only 60% for the wild-type ELVd-(+)-AUA hammerhead (Figure 3A). A similar trend in the rate constants was observed when the magnesium concentration was increased moderately (50 μM): ELVd-(+)-AUC≈ELVd-(+)-GUC>ELVd-(+)-GUA>ELVd-(+)-AUA, with the fraction of self-cleaved molecules at the end-point of the reaction being higher than 95% in all cases (Figure 3B). At higher magnesium concentration (500 μM), the self-cleavage rates were too fast to be analyzed manually (self-cleavage was essentially complete after 30 s, data not

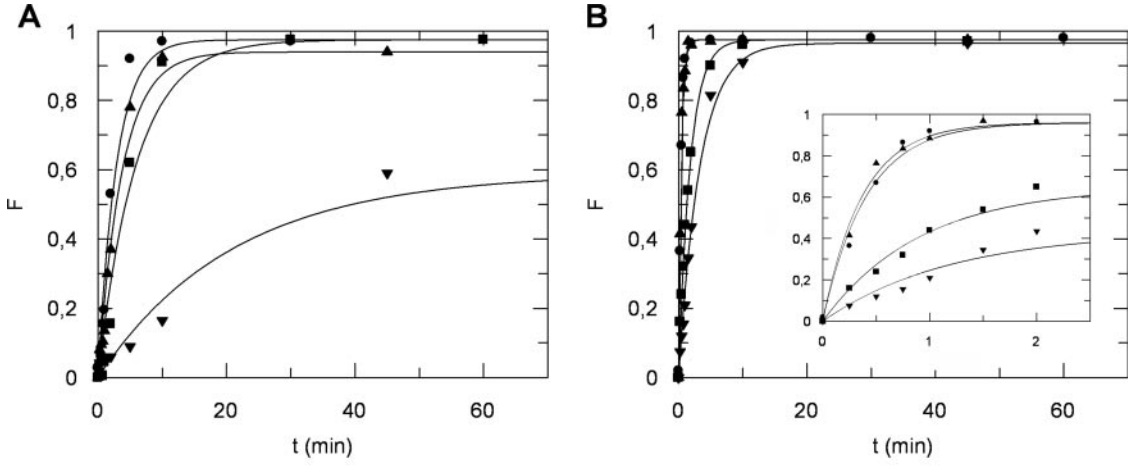


| | $k_{cat}$ (min$^{-1}$) | |
|---|---|---|
| | 10 μM $MgCl_2$ | 50 μM $MgCl_2$ |
| ▼ HH ELVd (+) AUA (wt) | 0,05 ± 0,007 (59%) | 0,30 ± 0,014 (96,5%) |
| ▲ HH ELVd (+) GUC | 0,27 ± 0,023 (94%) | 2,63 ± 0,122 (97,5%) |
| ● HH ELVd (+) AUC | 0,35 ± 0,042 (97,5%) | 2,34 ± 0,124 (98%) |
| ■ HH ELVd (+) GUA | 0,17 ± 0,026 (97,5%) | 0,56 ± 0,012 (97%) |

**Figure 3.** Representative self-cleavage kinetics at 10 μM (**A**) and 50 μM (**B**) magnesium of the purified wild-type ELVd (+) hammerhead and of three mutants affecting the trinucleotide preceding the self-cleavage site. The fraction of product at different times ($F_t$) was determined by radioactivity quantitation of the corresponding gel bands with a bioimage analyzer and fitted to the equation $F_t = F_\infty (1-e^{-kt})$, where $F_\infty$ is the fraction of product at the endpoint of the reaction and $k$ the first order rate constant of cleavage ($k_{cat}$). The inset displays the first 2 min for each experiment. The mean values obtained for the rate constants of the four hammerheads and for $F_\infty$ (between parenthesis) are shown below. The concentration of Mg was ∼1000-fold higher than that of hammerheads.

shown). Altogether these results indicate that the effects of changes in the trinucleotide preceding the self-cleavage site follow the same tendency observed previously in artificial *trans*-acting hammerheads under high magnesium concentration (38–41). However, they neither provide hints on why some catalytically sub-optimal trinucleotides like AUA have been selected in natural hammerheads, nor on why the catalytically most favorable trinucleotide AUC has been essentially excluded in natural hammerheads.

### Co- and post-transcriptional self-cleavage may be different: a model for the lack of the trinucleotide AUC in most natural hammerheads

Because RNA folding occurs during transcription (42), we considered the possibility that certain trinucleotides preceding the self-cleavage site, particularly AUC, might promote the transient adoption of catalytically-inactive metastable structures. If these metastable structures are indeed formed (see Discussion and Supplementary Figure S1), we reasoned that they could be indirectly revealed by their differential effect on self-cleavage very early during transcription, whereas the differences would be attenuated late in transcription when the most stable catalytically-active hammerhead outcompetes the metastable structures. The experimental data (Figure 4) are consistent with this model. Self-cleavage of the ELVd-(+)-AUC hammerhead during the initial transcription instants (15 s) was significantly lower than that of the other three ELVd hammerheads (22 versus 46–67%), whereas later in transcription (1.5 min) the differences were less conspicuous (78 versus 89–91%), with self-cleavage being very similar for the four ELVd hammerheads (89–94%) 10 min after initiating transcription (Figure 4A). Analogous results were obtained in independent experiments in which the magnesium concentration of the *in vitro* transcription mixture was, instead of 2 mM, 1 or 4 mM (data not shown). Following the approach for estimation of the self-cleavage rate constants during *in vitro* transcription (22), the values obtained for the four ELVd (+) hammerheads (at 2 mM magnesium and pH 8) were: ELVd-(+)-GUA> ELVd-(+)-AUA>ELVd-(+)-GUC>ELVd-(+)-AUC (Figure 4B). During *in vivo* transcription the differences could be even higher because interactions with host proteins forming part of the replication complex might stabilize the metastable structures, thus explaining why the trinucleotide AUC, the catalytically most favorable in a post-transcriptional context, is essentially absent in natural hammerheads.

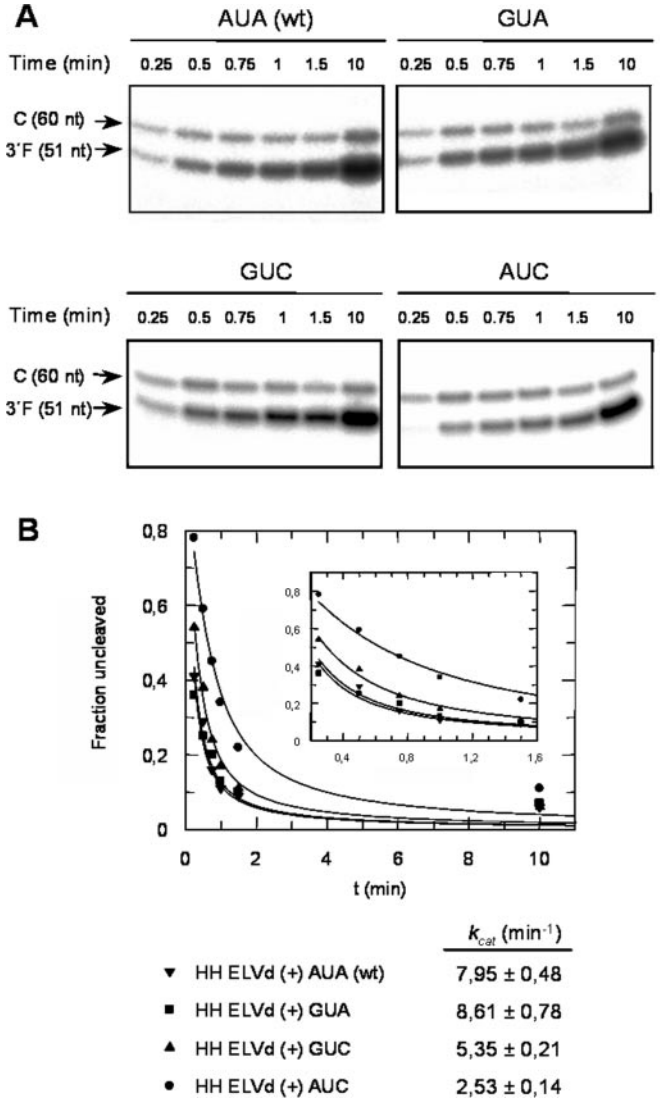


**Figure 4.** (**A**) Representative self-cleavage kinetics during transcription of the wild-type ELVd (+) hammerhead and of three mutants affecting the trinucleotide preceding the self-cleavage site. Transcriptions (at pH 8 and 2 mM $MgCl_2$) were made in the absence of the antisense oligodeoxyribonucleotides. Reaction aliquots were removed at different time intervals, quenched with an excess of stop solution, separated by PAGE in 15% gels containing 8 M urea, and revealed and quantitated by a bioimage analyzer. Positions of the complete (C) primary transcript and of the resulting self-cleavage 3′ fragment (3′F), with their sizes in nt are indicated on the left. The smaller self-cleavage 5′ fragment (9 nt) has migrated out of the gel. (**B**) Quantitative data were fitted to the equation derived previously (22) by a least square method. The inset displays the first 1.5 min for each experiment.

### Comparative analysis with other natural hammerheads reveals two ELVd (+) hammerhead derivatives as the catalytically most active at low magnesium concentration

To have a reliable estimate of the catalytic properties of the ELVd (+) hammerheads in relation to other known natural hammerheads, a self-cleavage kinetics analysis of the PLMVd (+), CChMVd (+) and sTRSV (+) hammerheads was performed at the same low magnesium concentrations. The morphology of these three hammerheads presents differences in the helices and loops but the trinucleotide preceding their self-cleavage sites is GUC (Figure 1C). At 10 μM magnesium, the self-cleavage rate constants of the PLMVd (+) and CChMVd (+) hammerheads were 5- to 6-fold lower than the comparable ELVd-(+)-GUC hammerhead (the ELVd variant with the same triplet preceding the self-cleavage site), whereas the self-cleavage rate constant of the sTRSV (+) hammerhead was negligible (Figure 5A). When compared with the fraction of self-cleaved molecules for the ELVd-(+)-GUC hammerhead at the end-point of the reaction (94%), the corresponding values for CChMVd (+) and, particularly, for the PLMVd (+) hammerheads were significantly lower (80 and 52%, respectively). At 50 μM magnesium

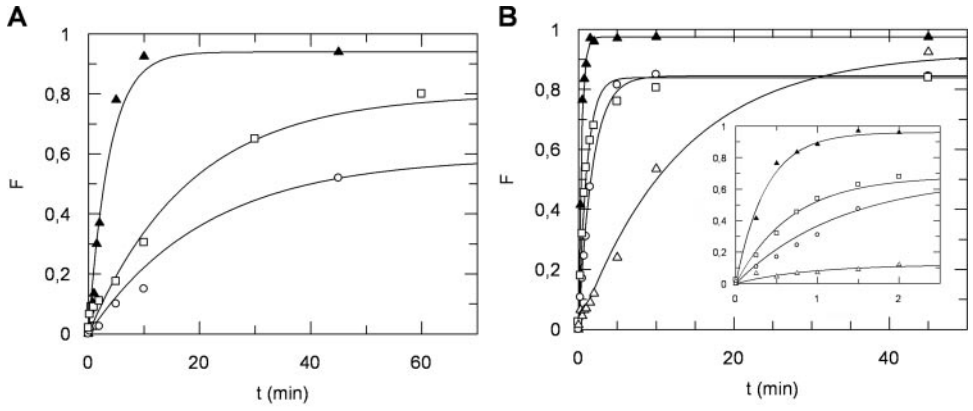


| | $k_{cat}$ (min$^{-1}$) | |
|---|---|---|
| | 10 μM $MgCl_2$ | 50 μM $MgCl_2$ |
| ▲ HH ELVd (+) GUC | 0,27 ± 0,023 (94%) | 2,63 ± 0,122 (97,5%) |
| ○ HH PLMVd (+) | 0,04 ± 0,008 (52%) | 0,57 ± 0,043 (84,5%) |
| □ HH CChMVd (+) | 0,06 ± 0,006 (80%) | 0,96 ± 0,049 (84%) |
| △ HH sTRSV (+) | ND | 0,08 ± 0,005 (92,5%) |

**Figure 5.** Representative self-cleavage kinetics at 10 μM (**A**) and 50 μM (**B**) magnesium of the purified ELVd-(+)-GUC mutant hammerhead and of three other natural hammerheads with the trinucleotide GUC preceding the self-cleavage site. The fraction of product at different times ($F_t$) was determined by radioactivity quantitation of the corresponding gel bands with a bioimage analyzer and fitted to the equation $F_t = F_\infty(1-e^{-kt})$, where $F_\infty$ is the fraction of product at the endpoint of the reaction and $k$ the first order rate constant of cleavage ($k_{cat}$). The inset displays the first 2 min for each experiment. The mean values obtained for the rate constants of the four hammerheads and for $F_\infty$ (between parenthesis) are shown below. ND, not detectable self-cleavage. The concentration of Mg was ~1000-fold higher than that of hammerheads.

the differences became somewhat diminished but the rate constant and the extent of self-cleavage of the ELVd-(+)-GUC hammerhead were still the highest (Figure 5B). Therefore, the latter hammerhead, and the ELVd-(+)-AUC mutant (Figure 3), appear as the catalytically most active in this particular post-transcriptional context.

## DISCUSSION

The study of hammerheads in their *cis* context and at the low magnesium concentration existing *in vivo* has still received limited interest, despite its implications for a better understanding of the catalytic mechanism and biological diversity of natural hammerheads, as well as for the development of artificial *trans*-acting hammerheads with increased activity in physiological conditions. Here we have examined the self-cleavage kinetics at low magnesium concentration of the hammerheads described recently in ELVd (20) and, from the effects of changes in the trinucleotide preceding the self-cleavage site, we have tried to derive some clues about the rules governing the limited variability of this trinucleotide in natural hammerheads.

Starting from the ELVd (+) hammerhead, with an AUA trinucleotide preceding the self-cleavage site, we changed this trinucleotide into GUC. Due to the very similar morphology of both ELVd hammerheads (Figure 1B), this substitution transformed the ELVd (+) hammerhead in a derivative analogous to the ELVd (−) hammerhead. Kinetic analysis at two low magnesium concentrations (10 and 50 μM) showed that the self-cleavage rate constant of the ELVd-(+)-GUC mutant was considerably higher than that of ELVd-(+)-AUA wild-type (Figure 3), raising the question of why two trinucleotides have been differentially selected in the two ELVd hammerheads. Moreover, under the same magnesium concentrations, the self-cleavage rate constants of the ELVd-(+)-AUC and ELVd-(+)-GUA mutants were similar to and somewhat lower than those of the ELVd-(+)-GUC mutant, respectively. Whereas the GUA trinucleotide precedes the self-cleavage site of two natural hammerheads (Table 1), why the catalytically very favorable trinucleotide AUC has been excluded in most natural hammerheads?

The effect of the trinucleotide preceding the self-cleavage site on the rate constant has been previously studied in several artificial *trans*-acting hammerheads at high magnesium concentration. Although there are some discrepancies that probably reflect the distinct characteristics of specific hammerheads, the highest self-cleavage rate constants were observed for the trinucleotides GUC and AUC, whereas those for the trinucleotides GUA and AUA were significantly smaller (38–41). These results parallel those reported here at low magnesium concentration with the *cis*-acting ELVd (+) hammerhead and its mutants, indicating that they are to a good extent independent of the *cis* or *trans* context.

In the framework of ELVd replication, the two trinucleotides preceding the self-cleavage site may have been differentially selected in the two hammerheads because of the need of differential self-cleavage rates during transcription of (+) and (−) strands. Replication additionally entails subsequent ligation of the self-cleaved RNAs. It is not yet clear whether in hammerhead viroids of the family *Avsunviroidae* this is an enzyme-catalyzed reaction or it occurs non-enzymatically (self-ligation) giving rise to a 2′,5′-phosphodiester bond [see (4) for a Discussion], but the RNA structures promoting self-cleavage and ligation may well be not be the same and, consequently, the trinucleotides preceding the self-cleavage

site may have an additional role in ligation. It is even possible that the higher rate and extent of ligation observed in a natural hammerhead with the interactions between loops 1 and 2 preserved could be relevant in physiological conditions (43), and that the trinucleotide preceding the self-cleavage/ligation site may have some influence. Moreover, in natural contexts this trinucleotide might play functional roles other than in cleavage and ligation. This is illustrated by the case of CChMVd, in which the (+) hammerhead has an extra A (A10) between the conserved A9 and the quasi-conserved G10.1. A10 causes a moderate decrease of the *trans*-cleaving rate constant with respect to the CChMVd (+) hammerhead without this residue, but because A10 also occupies a singular and indispensable position in the global CChMVd conformation as revealed by bioassays (44), these results show that some hammerheads deviate from the consensus due to the involvement of certain residues in critical function(s) other than self-cleavage.

However, whereas the above arguments can explain why some catalytically sub-optimal trinucleotides have been selected in natural hammerheads, the reasons excluding the catalytically most favorable trinucleotide AUC in almost all natural hammerheads are probably different. We believe that this exclusion can be accounted by considering that self-cleavage during transcription and in a protein-free medium may be different. Following transcription of the first hammerhead nucleotides, they can be kinetically trapped in a catalytically-inactive structure. These structures, predicted for the ELVd-(+)-AUC, ELVd-(+)-GUC, ELVd-(+)-GUA, and ELVd-(+)-AUA hammerheads with the Kinefold program (45) (Supplementary Figure S1), show that some trinucleotides preceding the self-cleavage site can potentially base pair with the CUGAU motif (hammerhead positions 3–7) (Figure 6). Moreover, the resulting interactions have different stability, with that formed by the trinucleotide AUC displaying the highest and, as a consequence, delaying self-cleavage. This model also explains why when in natural hammerheads the first nucleotide of the trinucleotide is A, the third must be also A (G is excluded because it would base pair with C3 and impede its role in the catalytic pocket, and U is also excluded because it can not form the complex array of non-canonical interactions) (11,16). Once transcription of the hammerhead is completed, the kinetic trap can be released as a result of the alternative interactions that can be formed (Figure 6), and the hammerhead can adopt its catalytically-active folding. Formation of the kinetic trap may be particularly facilitated in certain natural hammerheads, like the ELVd (+) hammerhead, with a long and stable helix I. It is

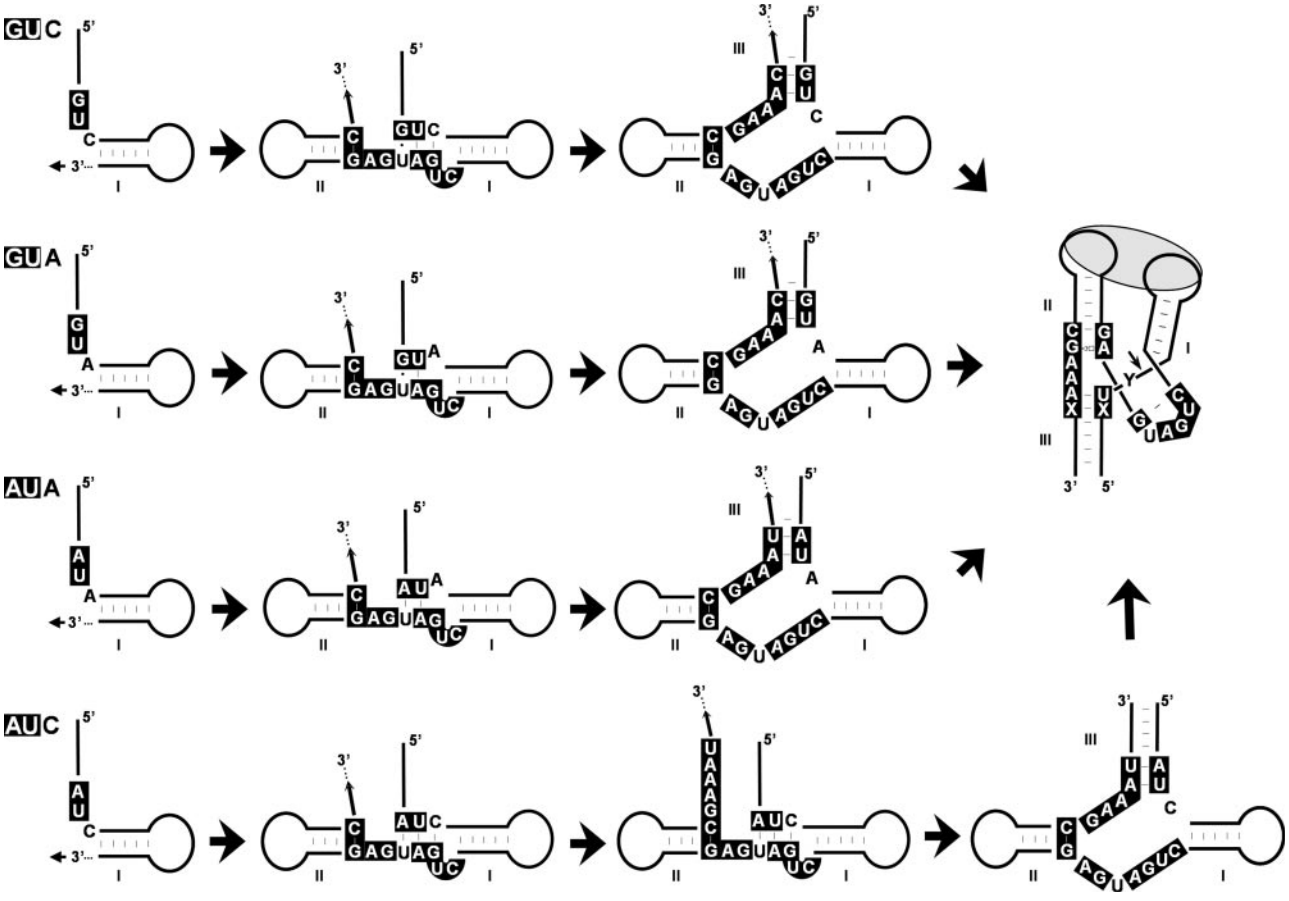


**Figure 6.** Model for the transient folding of four hammerheads with different trinucleotides preceding the self-cleavage site. During transcription, nucleotides forming part of the hammerhead catalytic core (in dark background) can be transiently involved in catalytically-inactive metastable structures. The higher stability of the structure with the trinucleotide AUC preceding the self-cleavage site can specifically delay the adoption of the catalytically-active hammerhead. In the scheme of the catalytically-active hammerhead (right) the pair X–X represents C–G or U–A, and the Y represents C or A.

also interesting to note that, in nature, an AUC trinucleotide preceding the self-cleavage site has been only found in the *Schistosome douthitti* hammerhead, whereas this trinucleotide is GUC in the other *Schistosome* spp. hammerheads deposited in databases. Due to the particular morphology of this hammerhead, adoption of a catalytically-inactive metastable structure cannot be facilitated by helix I because one of its strands is transcribed subsequently to all the other sequences forming the hammerhead. In summary, co- and post-transcriptional self-cleavage, particularly *in vivo,* may be different, with natural hammerheads having been probably selected through evolution to function under conditions for co-transcriptional self-cleavage. Hence, a deeper understanding of hammerheads (and probably other ribozymes) in their natural RNA context requires kinetic analysis not only in the *cis*-cleaving format but also during transcription. Pertinent to this point is the finding that transcription initiation of viroid strands occurs at specific sites, the location of which in the nascent strands is consistent with avoiding structures that disfavor the adoption of the catalytically-active hammerheads (46,47).

Finally, the kinetics analysis here reported also shows that the ELVd-(+)-GUC hammerhead presents the highest rate constant and extent of self-cleavage (in low magnesium and in a post-transcriptional context) when compared with three other natural hammerheads from two viroids and one satellite RNA in which the trinucleotide preceding the self-cleavage site is also GUC. This may be the result of the high thermodynamic stability of the helices of the ELVd-(+)-GUC hammerhead that would facilitate the tertiary interactions between the peripheral regions important for catalysis. Therefore, this hammerhead, and the ELVd-(+)-AUC mutant, can serve as a base for designing new and efficient *trans*-acting hammerheads in which the tertiary interactions are preserved.

## SUPPLEMENTARY DATA

Supplementary Data are available at NAR Online.

## ACKNOWLEDGEMENTS

This work has been partially supported by grants BFU2005-06808/BMC from the Ministerio de Educación y Ciencia (MEC) and ACOMP06/141 from the Generalidad Valenciana (Spain). A.C. has been supported by a pre-doctoral fellowship from the MEC, M.D.P. by a long-term postdoctoral fellowship of the International Human Frontier Science Program Organization and by a 'Ramón y Cajal' contract from the MEC, and S.G. by a postdoctoral fellowship from the Fundación 'José y Ana Royo' and by an I3P contract from the Consejo Superior de Investigaciones Científicas. Funding to pay the Open Access publication charges for this article was provided by the MEC.

*Conflict of interest statement*. None declared.

## REFERENCES

1. Hutchins,C.J., Rathjen,P.D., Forster,A.C. and Symons,R.H. (1986) Self-cleavage of plus and minus RNA transcripts of avocado sunblotch viroid. *Nucleic Acids Res*., **14**, 3627–3640.
2. Prody,G.A., Bakos,J.T., Buzayan,J.M., Schneider,I.R. and Bruening,G. (1986) Autolytic processing of dimeric plant virus satellite RNA. *Science*, **231**, 1577–1580.
3. Flores,R., Hernández,C., De la Peña,M., Vera,A. and Daròs,J.A. (2001) Hammerhead ribozyme structure and function in plant RNA replication. *Methods Enzymol*., **341**, 540–552.
4. Flores,R., Hernández,C., Martínez de Alba,E., Daròs,J.A. and Di Serio,F. (2005) Viroids and viroid-host interactions. *Ann. Rev. Phytopathol*., **43**, 117–139.
5. Forster,A.C. and Symons,R.H. (1987) Self-cleavage of plus and minus RNAs of a virusoid and a structural model for the active sites. *Cell*, **49**, 211–220.
6. Forster,A.C. and Symons,R.H. (1987) Self-cleavage of virusoid RNA is performed by the proposed 55-nucleotide active site. *Cell*, **50**, 9–16.
7. Pley,H.W., Flaherty,K.M. and McKay,D.B. (1994) Three-dimensional structure of a hammerhead ribozyme. *Nature*, **372**, 68–74.
8. Scott,W.G., Finch,J.T. and Klug,A. (1995) The crystal structure of an all-RNA hammerhead ribozyme: a proposed mechanism for RNA catalytic cleavage. *Cell*, **81**, 991–1002.
9. Scott,W.G., Murray,J.B., Arnold,J.R., Stoddard,B.L. and Klug,A. (1996) Capturing the structure of a catalytic RNA intermediate: the hammerhead ribozyme. *Science*, **274**, 2065–2069.
10. Rossi,J.J. and Couture,L.A. (eds) (1999) *Intracellular Ribozyme Applications: Principles and Protocols*. Horizon Scientific Press, Wymondham, UK.
11. Blount,K.F. and Uhlenbeck,O.C. (2005) The structure-function dilemma of the hammerhead ribozyme. *Annu. Rev. Biophys. Biomol. Struct*., **34**, 415–440.
12. De la Peña,M., Gago,S. and Flores,R. (2003) Peripheral regions of natural hammerhead ribozymes greatly increase their self-cleavage activity. *EMBO J*., **22**, 5561–5570.
13. Khvorova,A., Lescoute,A., Westhof,E. and Jayasena,S.D. (2003) Sequence elements outside the hammerhead ribozyme catalytic core enable intracellular activity. *Nature Struct. Biol*., **10**, 708–712.
14. Canny,M.D., Jucker,F.M., Kellogg,E., Khvorova,A., Jayasena,S.D. and Pardi,A. (2004) Fast cleavage kinetics of a natural hammerhead ribozyme. *J. Am. Chem. Soc*., **126**, 10848–10849.
15. Penedo,J.C., Wilson,T.J., Jayasena,S.D., Khvorova,A. and Lilley,D.M. (2004) Folding of the natural hammerhead ribozyme is enhanced by interaction of auxiliary elements. *RNA*, **10**, 880–888.
16. Martick,M. and Scott,W.G. (2006) Tertiary contacts distant from the active site prime a ribozyme for catalysis. *Cell*, **126**, 1–12.
17. Saksmerprome,V., Roychowdhury-Saha,M., Jayasena,S., Khvorova,A. and Burke,D.H. (2004) Artificial tertiary motifs stabilize trans-cleaving hammerhead ribozymes under conditions of submillimolar divalent ions and high temperatures. *RNA*, **12**, 1916–1924.
18. Weinberg,M.S. and Rossi,J.J. (2005) Comparative single-turnover kinetic analyses of trans-cleaving hammerhead ribozymes with naturally derived non-conserved sequence motifs. *FEBS Lett*., **579**, 1619–1624.
19. Burke,D.H. and Greathouse,S.T. (2005) Low-magnesium, trans-cleavage activity by type III, tertiary stabilized hammerhead ribozymes with stem 1 discontinuities. *BMC Biochem*., **6**, 14.
20. Fadda,Z., Daròs,J.A., Fagoaga,C., Flores,R. and Duran-Vila,N. (2003) Eggplant latent viroid (ELVd): candidate type species for a new genus within family *Avsunviroidae* (hammerhead viroids). *J. Virol*., **77**, 6528–6532.
21. Flores,R., Daròs,J.A. and Hernández,C. (2000) The *Avsunviroidae* family: viroids with hammerhead ribozymes. *Adv. Virus Res*., **55**, 271–323.
22. Long,D.M. and Uhlenbeck,O.C. (1994) Kinetic characterization of intramolecular and intermolecular hammerhead RNAs with stem II deletions. *Proc. Natl Acad. Sci. USA*, **91**, 6977–6981.
23. Woese,C.R., Winker,S. and Gutell,R.R. (1990) Architecture of ribosomal RNA: constraints on the sequence of 'tetra-loops'. *Proc. Natl Acad. Sci. USA*, **87**, 8467–8471.
24. Heus,H.A. and Pardi,A. (1991) Structural features that give rise to the unusual stability of RNA hairpins containing GNRA loops. *Science*, **253**, 191–194.
25. Hernández,C. and Flores,R. (1992) Plus and minus RNAs of peach latent mosaic viroid self cleave *in vitro* via hammerhead structures. *Proc. Natl Acad. Sci. USA*, **89**, 3711–3715.

26. Navarro,B. and Flores,R. (1997) Chrysanthemum chlorotic mottle viroid: unusual structural properties of a subgroup of viroids with hammerhead ribozymes. *Proc. Natl Acad. Sci. USA*, **94**, 11262–11267.
27. Miller,W.A., Hercus,T., Waterhouse,P.M. and Gerlach,W.L. (1991) A satellite RNA of barley yellow dwarf virus contains a novel hammerhead structure in the self-cleavage domain. *Virology*, **183**, 711–720.
28. Di Serio,F., Daròs,J.A., Ragozzino,A. and Flores,R. (1997) A 451-nt circular RNA from cherry with hammerhead ribozymes in its strands of both polarities. *J. Virol.*, **71**, 6603–6610.
29. Di Serio,F., Daròs,J.A., Ragozzino,A. and Flores,R. (2006) Close structural relationship between two hammerhead viroid-like RNAs associated with cherry chlorotic rusty spot disease. *Arch. Virol.*, **151**, 1539–1549.
30. Vaish,N.K., Heaton,P.A. and Eckstein,F. (1997) Isolation of hammerhead ribozymes with altered core sequences by in vitro selection. *Biochemistry*, **36**, 6495–6501.
31. Ambrós,S. and Flores,R. (1998) *In vitro* and *in vivo* self-cleavage of a viroid RNA with a mutation in the hammerhead catalytic pocket. *Nucleic Acids Res.*, **26**, 1877–1883.
32. Forster,A.C., Davies,C., Sheldon,C.C., Jeffries,A.C. and Symons,R.H. (1988) Self-cleaving viroid and newt RNAs may only be active as dimers. *Nature*, **334**, 265–267.
33. Miller,W.A. and Silver,S.L. (1991) Alternative tertiary structure attenuates self-cleavage of the ribozyme in the satellite RNA of barley yellow dwarf virus. *Nucleic Acids Res.*, **19**, 5313–5320.
34. Pabón-Peña,L.M., Zhang,Y. and Epstein,L.M. (1991) Newt satellite 2 transcripts self-cleave by using an extended hammerhead structure. *Mol. Cell Biol.*, **11**, 6109–6115.
35. Been,M.D. and Perrotta,A.T. (1995) Optimal self-cleavage activity of the hepatitis delta virus RNA is dependent on a homopurine base pair in the ribozyme core. *RNA*, **1**, 1061–1070.
36. Salehi-Ashtiani,K. and Szostak,J.W. (2001) *In vitro* evolution suggests multiple origins for the hammerhead ribozyme. *Nature*, **414**, 82–84.
37. Przybilski,R., Graf,S., Lescoute,A., Nellen,W., Westhof,E., Steger,G. and Hammann,C. (2005) Functional hammerhead ribozymes naturally encoded in the genome of *Arabidopsis thaliana*. *Plant Cell*, **17**, 1877–1885.
38. Ruffner,D.E., Stormo,G.D. and Uhlenbeck,O.C. (1990) Sequence requirements of the hammerhead RNA self-cleavage reaction. *Biochemistry*, **29**, 10695–10702.
39. Nakamaye,K.L. and Eckstein,F. (1994) AUA-cleaving hammerhead ribozymes: attempted selection for improved cleavage. *Biochemistry*, **33**, 1271–1277.
40. Zoumadakis,M. and Tabler,M. (1995) Comparative analysis of cleavage rates after systematic permutation of the NUX consensus target motif for hammerhead ribozymes. *Nucleic Acids Res.*, **23**, 1192–1196.
41. Shimayama,T., Nishikawa,S. and Taira,K. (1995) Generality of the NUX rule: kinetic analysis of the results of systematic mutations in the trinucleotide at the cleavage site of hammerhead ribozymes. *Biochemistry*, **34**, 3649–3654.
42. Mahen,E.M., Harger,J.W., Calderon,E.M. and Fedor,M.J. (2005) Kinetics and thermodynamics make different contributions to RNA folding *in vitro* and in yeast. *Mol Cell*, **19**, 27–37.
43. Nelson,J.A., Shepotinovskaya,I. and Uhlenbeck,O.C. (2005) Hammerheads derived from sTRSV show enhanced cleavage and ligation rate constants. *Biochemistry*, **44**, 14577–14585.
44. De la Pena,M. and Flores,R. (2001) An extra nucleotide in the consensus catalytic core of a viroid hammerhead ribozyme: implications for the design of more efficient ribozymes. *J. Biol. Chem.*, **276**, 34586–34593.
45. Xayaphoummine,A., Bucher,T. and Isambert,H. (2005) Kinefold web server for RNA/DNA folding path and structure prediction including pseudoknots and knots. *Nucleic Acid Res.*, **33**, 605–610.
46. Navarro,J.A. and Flores,R. (2000) Characterization of the initiation sites of both polarity strands of a viroid RNA reveals a motif conserved in sequence and structure. *EMBO J.*, **19**, 2662–2670.
47. Delgado,S., Martínez de Alba,E., Hernández,C. and Flores,R. (2005) A short double-stranded RNA motif of peach latent mosaic viroid contains the initiation and the self-cleavage sites of both polarity strands. *J. Virol.*, **79**, 12934–12943.